Superplastic Constitutive Equation Including Percentage of High-Angle Grain Boundaries as a Microstructural Parameter

K. WANG, F.C. LIU, P. XUE, D. WANG, B.L. XIAO, and Z.Y. MA

Fifteen Al-Mg-Sc samples with subgrain/grain sizes in the range of 1.8 to 4.9 μm were prepared through the processing methods of friction stir processing (FSP), equal-channel-angular pressing (ECAP), rolling, annealing, and combinations of the above. The percentages of high-angle grain boundaries (HAGBs) of these fine-grained alloys were distributed from 39 to 97 pct. The samples processed through FSP had a higher percentage of HAGBs compared to other samples. Superplasticity was achieved in all fifteen samples, but the FSP samples exhibited better superplasticity than other samples because their fine equiaxed grains, which were mostly surrounded by HAGBs, were conducive to the occurrence of grain boundary sliding (GBS) during superplastic deformation. The dominant deformation mechanism was the same for all fifteen samples, *i.e.,* GBS controlled by grain boundary diffusion. However, the subgrains were the GBS units for the rolled or ECAP samples, which contained high percentages of unrecrystallized grains, whereas the fine grains were the GBS units for the FSP samples. Superplastic data analysis revealed that the dimensionless A in the classical constitutive equation for superplasticity of fine-grained Al alloys was not a constant, but increased with an increase in the percentage of HAGBs, demonstrating that the enhanced superplastic deformation kinetics can be ascribed to the high percentage of HAGBs. A modified superplastic constitutive equation with the percentage of HAGBs as a new microstructural parameter was established.

DOI: 10.1007/s11661-015-3230-8

I. INTRODUCTION

SUPERPLASTICITY refers to the ability of materials to exhibit high uniform elongation when pulled in tension while maintaining a stable microstructure.[1] This phenomenon has considerable industrial potential for the manufacture of complex sheet structures. It has been widely accepted that the constitutive relationship for superplasticity can be expressed in the following generalized form:[2]

$$\dot{\varepsilon} = A\frac{D_0 Eb}{kT}\exp\left(-\frac{Q}{RT}\right)\left(\frac{b}{d}\right)^p\left(\frac{\sigma-\sigma_0}{E}\right)^n, \qquad [1]$$

where $\dot{\varepsilon}$ is the strain rate, A is a dimensionless value, D_0 is the pre-exponential constant for diffusivity, E is Young's modulus, b is Burger's vector, k is Boltzmann's constant, T is the absolute temperature, Q is the activation energy dependent on the rate-controlling process, R is the gas constant, d is the inverse grain size, p is the grain size exponent, σ is the applied stress, σ_0 is the threshold stress, and n is the stress exponent.

The superplastic data analysis for a large number of powder metallurgy-processed Al-based alloys demonstrated that the activation energies were close to that for the grain boundary diffusion of Al (84 kJ/mol), the inverse grain size dependence p and the stress exponent n were equal to 2 in Eq. [1], and the dimensionless value, A, was previously considered to be less than 50.[3–5]

Equation [1] shows that for the classical constitutive equation, the grain size is the sole microstructural determining parameter of the superplastic properties, and therefore, grain refinement is considered to be the sole method for increasing the superplastic deformation rate or reducing deformation temperature. Therefore, many processing methods,[6,7] such as equal channel angular pressing (ECAP),[8] high-pressure torsion (HPT),[9] cold rolling,[10] and friction stir processing (FSP),[11] were used to refine the grains of various alloys

K. WANG, formerly Research Fellow with the Shenyang National Laboratory for Materials Science, Institute of Metal Research, Chinese Academy of Sciences, 72 Wenhua Road, Shenyang 110016, P.R. China, is now Associate Professor with College of Materials Science and Engineering, Chongqing University, 174 Shapinba Main Street, Chongqing 400030, P.R. China. F.C. LIU, formerly Postgraduate with the Shenyang National Laboratory for Materials Science, Institute of Metal Research, Chinese Academy of Sciences, is now Research Fellow with the Department of Mechanical Engineering, Brigham Young University, Provo, UT 84602. P. XUE, Assistant Professor, D. WANG, Associate Professor, and B.L. XIAO and Z.Y. MA, Professors, are with the Shenyang National Laboratory for Materials Science, Institute of Metal Research, Chinese Academy of Sciences. Contact email: zyma@imr.ac.cn

K. Wang and F.C. Liu have contributed equally to this work and share first authorship.

Manuscript submitted February 28, 2015.
Article published online November 16, 2015

in order to shift the optimum superplastic deformation to a lower temperature and/or higher strain rate.[12–14]

Generally, the grain size needs to be reduced to less than 1 μm to obtain excellent high-strain-rate superplasticity (HSRS, optimum strain rates $\geq 1 \times 10^{-2}$ s^{-1}) for most of the Al alloys produced by conventional severe plastic deformation methods[15,16] due to the fact that a considerable fraction of grains in these alloys are partially surrounded by low-angle grain boundaries (LAGBs with misorientation between 2 deg and 15 deg). A typical example is that the ECAP Al-Mg-Sc alloy with a grain size of 0.2 μm exhibited a maximum elongation of 1560 pct at a high strain rate of 3.3×10^{-2} s^{-1}.[15] Comparatively, a maximum elongation of 2150 pct was obtained at an even higher strain rate of 1×10^{-1} s^{-1} in FSP Al-Mg-Sc alloy with a grain size of 2.6 μm.[16] Furthermore, many FSP Al alloys with grain sizes in the range of 1 to 10 μm have also exhibited excellent HSRS.[16–21] The optimum superplastic deformation rate for FSP 7075Al[20] was more than one order of magnitude higher than that for 7075Al processed by thermomechanical processing (TMP).[22] These phenomena cannot be completely explained by Eq. [1].

More importantly, through the superplastic data analysis of two FSP 7075Al samples with average grain sizes of 3.8 and 7.5 μm, Ma *et al.*[20] demonstrated that the dimensionless value A was as high as 790 for the FSP 7075Al, which is almost 20 times higher than the A value observed in powder metallurgy-processed Al alloys. Ma *et al.*[21] also found that the dimensionless value increased from about 40 in extruded Al-Mg-Zr to about 700 in the FSP Al-Mg-Zr. The high dimensionless values were subsequently observed in other FSP 7075Al and Al-Mg-Sc samples.[23–25] These results suggested that the enhanced superplastic deformation kinetics seems to be a common phenomenon in FSP Al alloys. Obviously, the classical constitutive equation cannot explain the significantly enhanced superplastic deformation kinetics in these fine-grained FSP Al alloys.

Thanks to the wide application of the electron backscattered diffraction (EBSD) technique in recent years, increasing information about the grain boundary characteristics of the fine-grained Al alloys can be obtained. It is noted that the percentage of high-angle grain boundaries (HAGBs with misorientation ≥15 deg) in the FSP Al alloys was in the range of 90 to 97 pct.[11,26] This value is significantly higher than that obtained in conventional TMP Al alloys with a typical ratio of 50 to 65 pct,[27,28] and higher than that in ECAP Al alloys with a ratio hardly higher than 80 pct.[17,29,30] It is supposed that the enhanced superplastic deformation kinetics in the FSP Al alloys should be ascribed to their high percentage of HAGBs because it is generally accepted that grain boundary sliding (GBS) can happen more easily along HAGBs than along LAGBs during superplastic deformation. However, a detailed investigation on this subject is still lacking.

Based on the above analysis, it seems that the dimensionless A is a variable associated with the percentage of HAGBs. In order to confirm this hypothesis, TMP, ECAP, and FSP as well as their combinations were used in this study to prepare fine-grained Al alloys with various percentages of HAGBs covering a wide range. All these fine-grained Al alloys were subjected to microstructural examination, superplastic testing, and superplastic data analysis. The aim of this study is (a) to elucidate the origin of enhanced superplastic deformation kinetics, (b) to establish the quantitative relationship between superplastic deformation kinetics and the percentage of HAGBs, and (c) to develop a modified superplastic constitutive equation that includes the percentage of HAGBs as another microstructural parameter.

II. EXPERIMENTAL

An Al-Mg-Sc ingot with a composition of Al-5.33Mg-0.23Sc-0.49Mn-0.14Fe-0.06Zr (wt pct) was initially homogenized at 703 K (430 °C) for 24 hours, and then was extruded into plates with an extrusion ratio of ~16 and a ram speed of 0.5 mm s^{-1}. The extruded plates with dimensions of 300 mm (length) × 70 mm (width) × 8 mm (thickness) were subjected to FSP and rolling. Rectangular blocks with dimensions of 130 mm (length) × 18 mm (width) × 8 mm (thickness) were cut from the extruded plates and then forged into blocks with section dimensions about 12 mm × 12 mm at 523 K (250 °C). The cylinders with dimensions of 100 mm (length) × 10 mm (diameter) were cut from the forged blocks for ECAP.

ECAP was performed at 723 K (450 °C) and a pressing speed of ~10 mm s^{-1} using a die with a channel angle of 90 deg and an additional angle of 45 deg at the outer arc of curvature where two channels intersect. An equivalent strain of ~1 was produced for each pass of ECAP through the die. The samples were rotated by 90 deg around their longitudinal axis in the same sense in each pass. Two FSP tools were used in this study. Tool 1 consisted of a shoulder 12 mm in diameter and a threaded cylindrical pin 4 mm in diameter and 4 mm in length. Tool 2 had a shoulder 20 mm in diameter and a threaded cylindrical pin 8 mm in diameter and 6.5 mm in length. An independent or a combination of the process of FSP, ECAP, and rolling was used in order to produce fine-grained samples with varied percentages of HAGBs. The processing details are listed in Figure 1.

Mini tensile specimens 2.5 mm in gauge length, 1.4 mm in gauge width, and 0.8 mm in gauge thickness were cut from the processed samples. For the TMP and ECAP samples, the tensile directions were parallel to the rolling and extrusion directions, respectively. For the FSP samples, the tensile directions were perpendicular to the FSP direction. All the tensile specimens were ground and polished using a 1-μm polishing paste before the tensile test. Constant crosshead speed tensile tests were conducted using an Instron 5848 micro-tester. Each specimen was held at the testing temperature for about 15 minutes in order to reach thermal equilibrium.

EBSD examination was performed on the gauge center of the mini tensile specimens, which were electrically polished to produce a strain-free surface. In order to provide the correct microstructure information just before superplastic deformation, the EBSD specimens were held at their optimum superplastic deformation

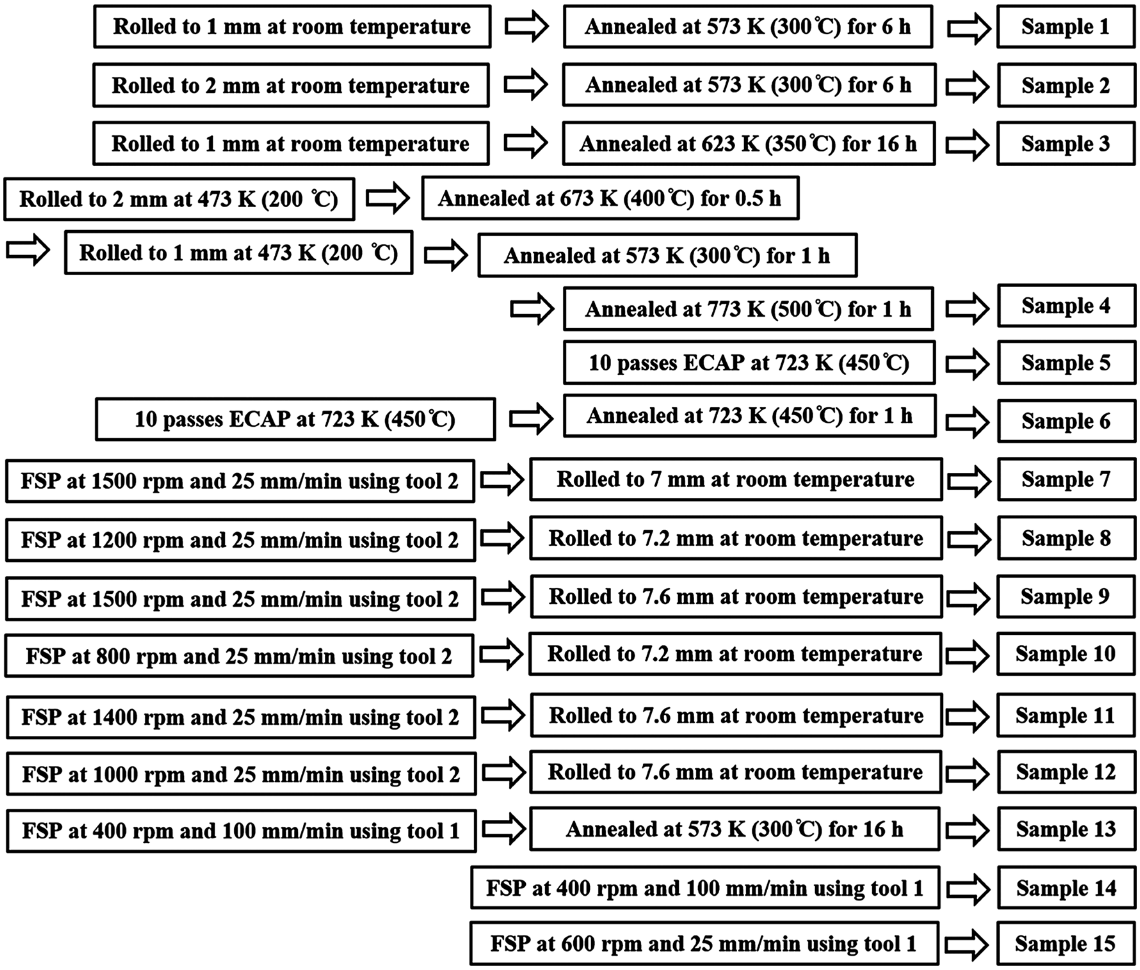

Fig. 1—Production processes of fine-grained Al-Mg-Sc samples.

temperatures for 15 minutes before being subjected to polishing. The EBSD maps were obtained using a ZEISS SUPRA 35 scanning electron microscope with a HKL OIM system operating with an accelerating voltage of 10 keV. The average subgrain/grain sizes were estimated by the linear intercept method.

III. RESULTS

A. *Microstructure of the Superplastic Materials*

EBSD examinations showed that the Al-Mg-Sc samples produced by different processing methods exhibited substantially different grain structures (Figure 2). In the EBSD maps, the HAGBs were depicted as dark lines, while the LAGBs were depicted as white lines. The lower limit of 2 deg was selected due to the resolution limit of the EBSD.[31] Four main microstructural characteristics were observed. Firstly, the samples processed by the combination of rolling and annealing (samples 1 to 4) contained a heavily deformed microstructure composed of largely irregular-shaped grains with many fine equiaxed subgrains separated by the LAGBs. Secondly, the samples processed by ECAP consisted of fine recrystallized grains and unrecrystallized large grains due to insufficient plastic deformation. Most of the large grains in the ECAP samples were also divided into fine equiaxed subgrains by the LAGBs (samples 5 and 6). Thirdly, the FSP samples processed at various parameters showed homogeneous microstructures consisting of fine equiaxed grains that differ mainly in the size of the grains (samples 7 to 15). Fourthly, the samples processed through ECAP or FSP contained more fine recrystallized grains than the samples mainly processed by rolling. This can be ascribed to the larger deformation or the higher deformation rate for the samples processed through ECAP or FSP.[11,32]

Table I shows that the average subgrain sizes for all the samples were determined to be below 5 μm, which is expected to favor GBS during high temperature deformation.

The misorientation angle histograms of the Al-Mg-Sc samples are shown in Figure 3. For comparison, the theoretical misorientation angle distribution for randomly oriented cubes predicted by Mackenzie[33] is given as the solid line in each figure. Two peaks in the LAGB and HAGB ranges were observed in the samples which involved rolling or ECAP (Figures 3(a) through (f)). Similar bimodal distribution was also extensively

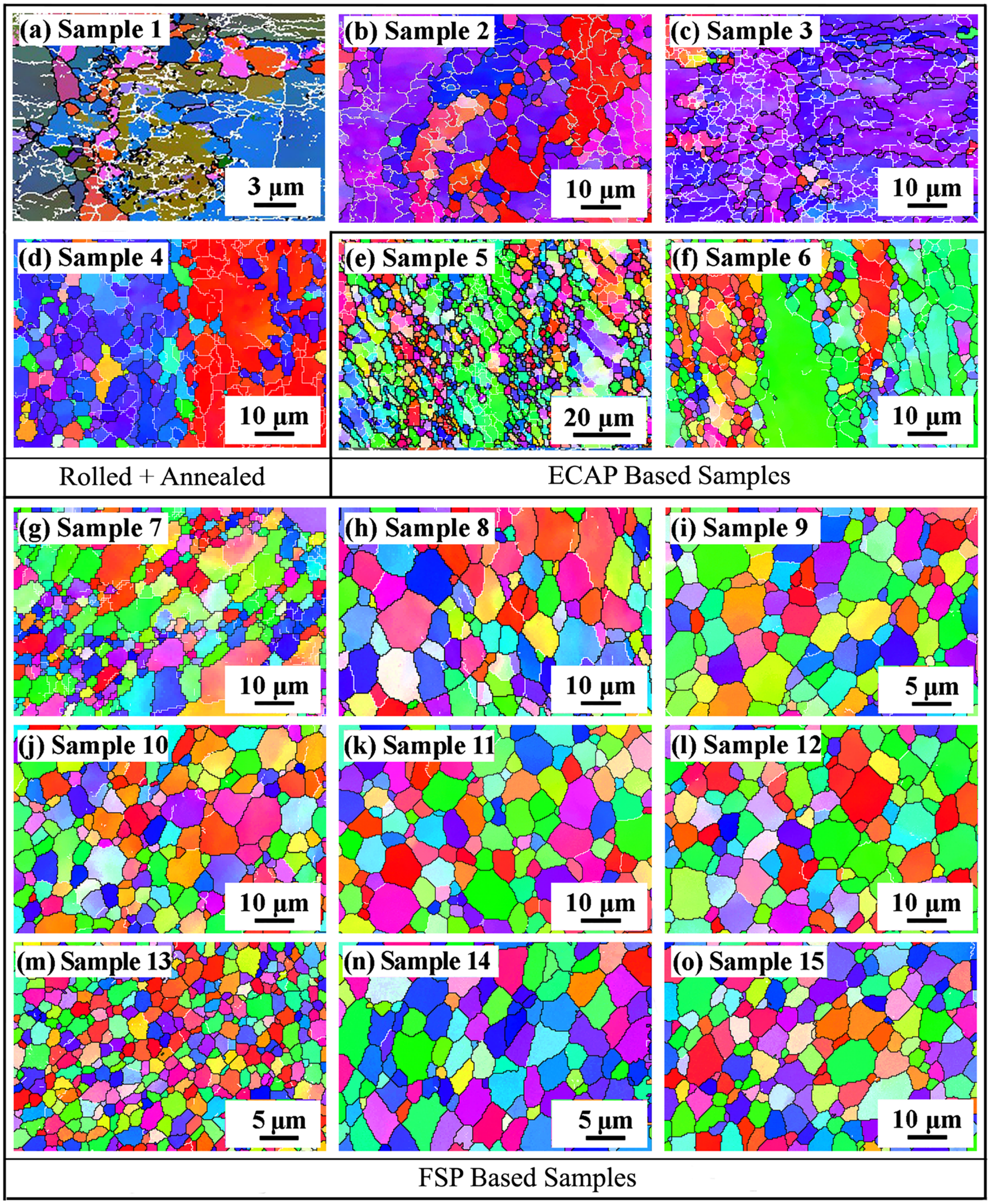

Fig. 2—EBSD micrographs of fine-grained Al-Mg-Sc samples processed by various processing methods (dark lines represent HAGBs, and white lines represent LAGBs).

Table I. Microstructural Characteristics of Fine-Grained Al-Mg-Sc Samples Produced by Various Processes

Samples	1	2	3	4	5	6	7	8	9	10	11	12	13	14	15
Subgrain/grain size (μm)	1.8	2.6	2.4	4.2	4.1	4.2	4.3	4.6	4.4	4.0	4.9	4.2	2.1	2.6	3.3
Percentage of HAGBs (pct)	39	48	53	50	65	64	78	83	89	90	92	93	95	96	97

observed in several fine-grained Al alloys prepared by other plastic deformation processes[7,32,34] due to the existence of a high percentage of both recrystallized and unrecrystallized grains. For the samples produced by FSP, the misorientation distribution matched well with the theoretical distribution. Table I shows that the

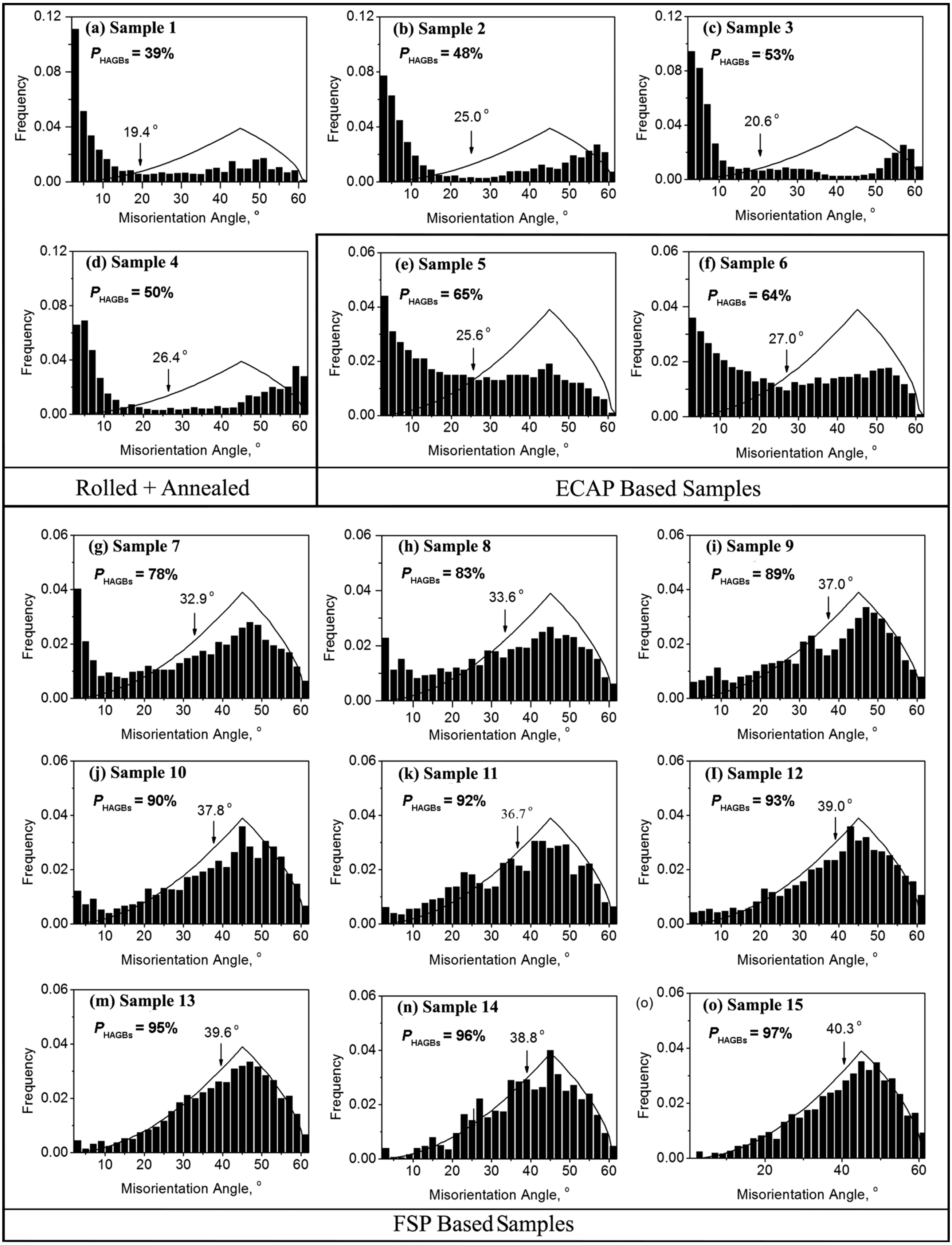

Fig. 3—Misorientation distribution of fine-grained Al-Mg-Sc samples processed by various processing methods.

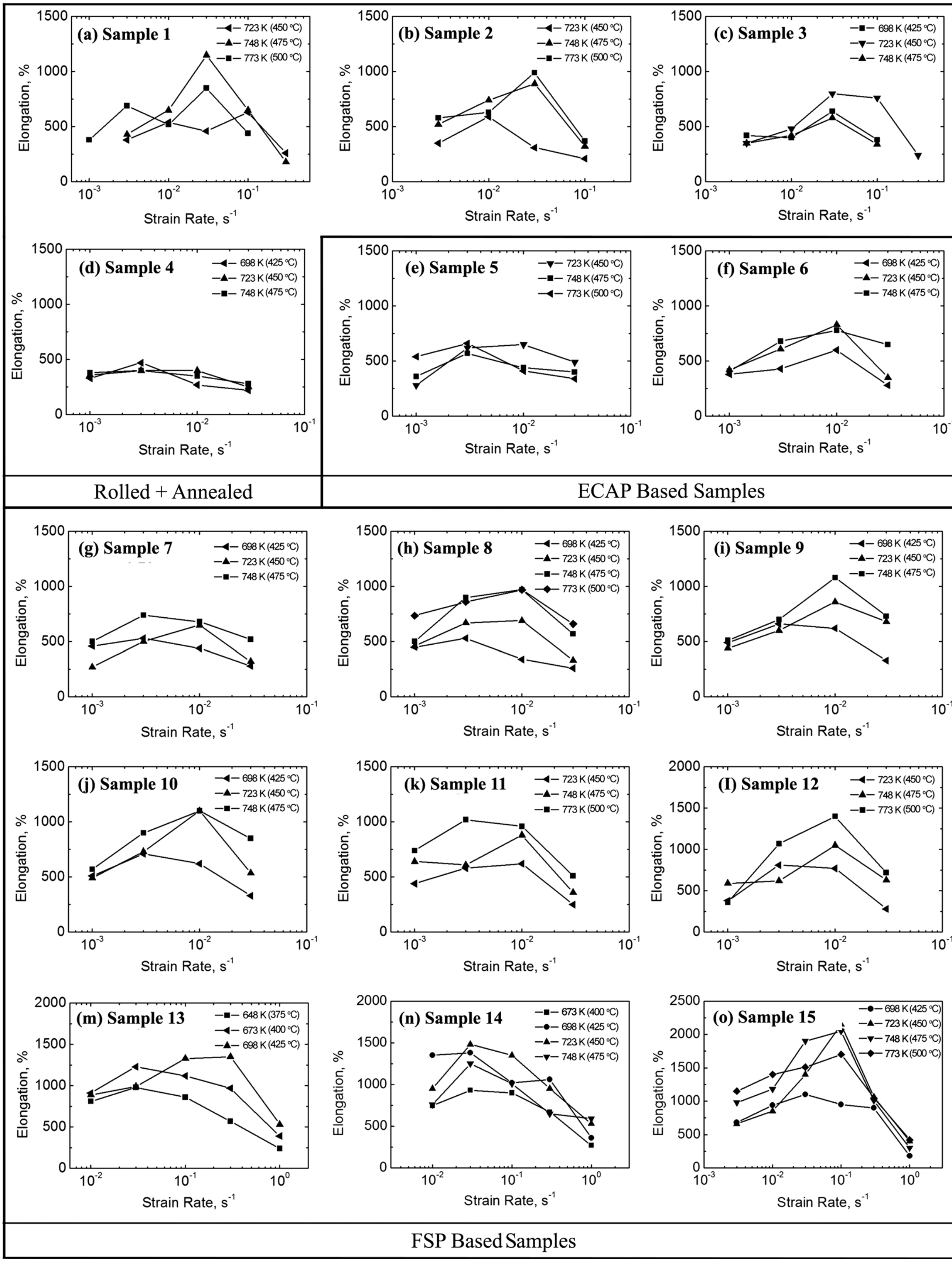

Fig. 4—Variation of elongation with initial strain rate at various test temperatures for fine-grained Al-Mg-Sc samples processed by various processing methods.

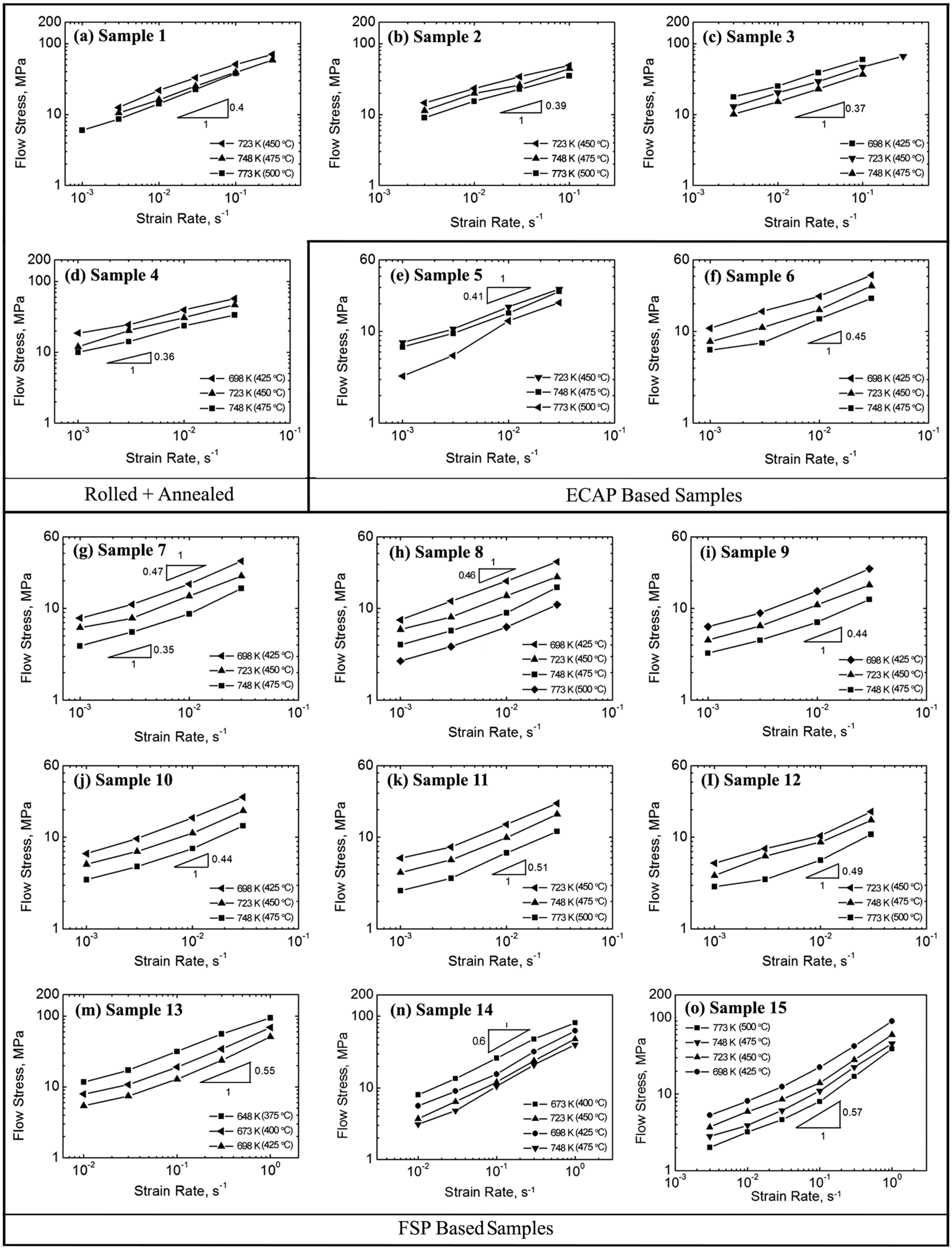

Fig. 5—Variation of flow stress with initial strain rate for fine-grained Al-Mg-Sc samples processed by various processing methods.

Table II. A Summary of Superplastic Properties of Fine-Grained Al-Mg-Sc Samples

Sample No.	Strain Rate Sensitivity	Deformation Conditions	Maximum Elongation (pct)	Percentage of HAGB (pct)	*A* Value
1	0.40	748 K (475 °C), 3×10^{-2} s^{-1}	1150	39	40
2	0.39	773 K (500 °C), 3×10^{-2} s^{-1}	990	48	70
3	0.37	723 K (450 °C), 3×10^{-2} s^{-1}	800	53	85
4	0.36	698 K (425 °C), 3×10^{-3} s^{-1}	470	50	88
5	0.41	723 K (450 °C), 1×10^{-2} s^{-1}	650	65	145
6	0.45	723 K (450 °C), 1×10^{-2} s^{-1}	830	64	150
7	0.35	748 K (475 °C), 3×10^{-3} s^{-1}	740	78	260
8	0.46	748 K (475 °C), 1×10^{-2} s^{-1}	970	83	335
9	0.44	748 K (475 °C), 1×10^{-2} s^{-1}	1080	89	390
10	0.44	748 K (475 °C), 1×10^{-2} s^{-1}	1100	90	350
11	0.51	773 K (500 °C), 1×10^{-3} s^{-1}	1050	92	420
12	0.49	773 K (500 °C), 1×10^{-2} s^{-1}	1400	93	460
13	0.55	698 K (425 °C), 3×10^{-1} s^{-1}	1350	95	670
14	0.60	723 K (450 °C), 3×10^{-2} s^{-1}	1480	96	990
15	0.57	723 K (450 °C), 1×10^{-1} s^{-1}	2150	97	1000

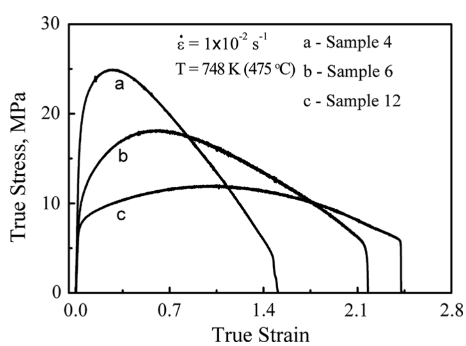

Fig. 6—Typical flow stresses for different samples deformed at sample temperature and strain rate.

percentage of HAGBs differed for each sample and was scattered over a wide range. Such a distribution is conducive to clarifying the relationship between the percentage of HAGBs and superplastic deformation kinetics.

B. *Superplastic Behavior*

Figure 4 shows the variation of superplastic elongation with initial strain rate for the Al-Mg-Sc samples processed by different processing methods. All the samples exhibited superplastic elongation higher than 500 pct at their optimum deformation conditions. Furthermore, HSRS was obtained in all the samples except samples 4 and 7. Especially, the optimum strain rate for sample 13 has reached 3×10^{-1} s^{-1}, which is extremely high for the superplastic deformation of Al alloys.

Previous studies have shown that the fine-grained Al-Mg-Sc alloys exhibited a slow and essentially uniform grain growth due to the presence of high density of fine Al_3Sc dispersoids both at the grain boundaries and within the grain interiors.[35] The fine and stable microstructure in the Al-Mg-Sc alloys is suitable to superplastic deformation at elevated temperatures. The samples processed by FSP exhibited higher optimal elongation than those processed by rolling and ECAP because the fine equiaxed and uniform grain structure in the FSP samples was beneficial to the occurrence of GBS during the initial superplastic deformation stage.[32]

Figure 5 shows the variation of flow stress (at true strain of 0.1) with the initial strain rate for all the Al-Mg-Sc samples. Consistent with general observation, the flow stress decreased as the deformation temperature was increased or the strain rate was reduced. For comparison, the maximum elongation, its corresponding strain rate sensitivity (*m* value), and the deformation condition for each sample are summarized in Table II. The *m* values were in the range of 0.35 to 0.6 for all samples, demonstrating the high contribution of GBS to the superplastic deformation. It is interesting to note that the *m* value tended to increase with an increase in the percentage of HAGBs, and the largest strain rate sensitivity was achieved in sample 14, which was produced by FSP.

Figure 6 shows the stress flow curves of samples 4, 6, and 12 deformed at 748 K (475 °C) and 1×10^{-2} s^{-1}. These three samples have the same grain size of 4.2 μm but different percentages of HAGBs. Sample 4, mainly processed through rolling and annealing, exhibited the highest maximum flow stress and the lowest elongation. Sample 6, mainly processed through ECAP, showed a medium maximum flow stress and a medium elongation. By comparison, the lowest maximum flow stress and the highest elongation were observed in the FSP sample (sample 12). These stress flow curves indicate that an increase in the percentage of HAGBs reduced the superplastic flow stress and increased the superplastic elongation.

Overall, all the Al-Mg-Sc samples processed by various processing methods exhibited high superplastic elongation and *m* values, which are the typical superplastic deformation characteristics. Compared to the other samples, the sample processed by the combination of rolling and annealing exhibited a lower elongation, a higher flow stress, and a narrower superplastic deformation window due to the high percentage of subgrain boundaries. The FSP samples were characterized by fine and equiaxed grains, which are ideal grain structures for superplasticity. Therefore, the FSP samples showed very

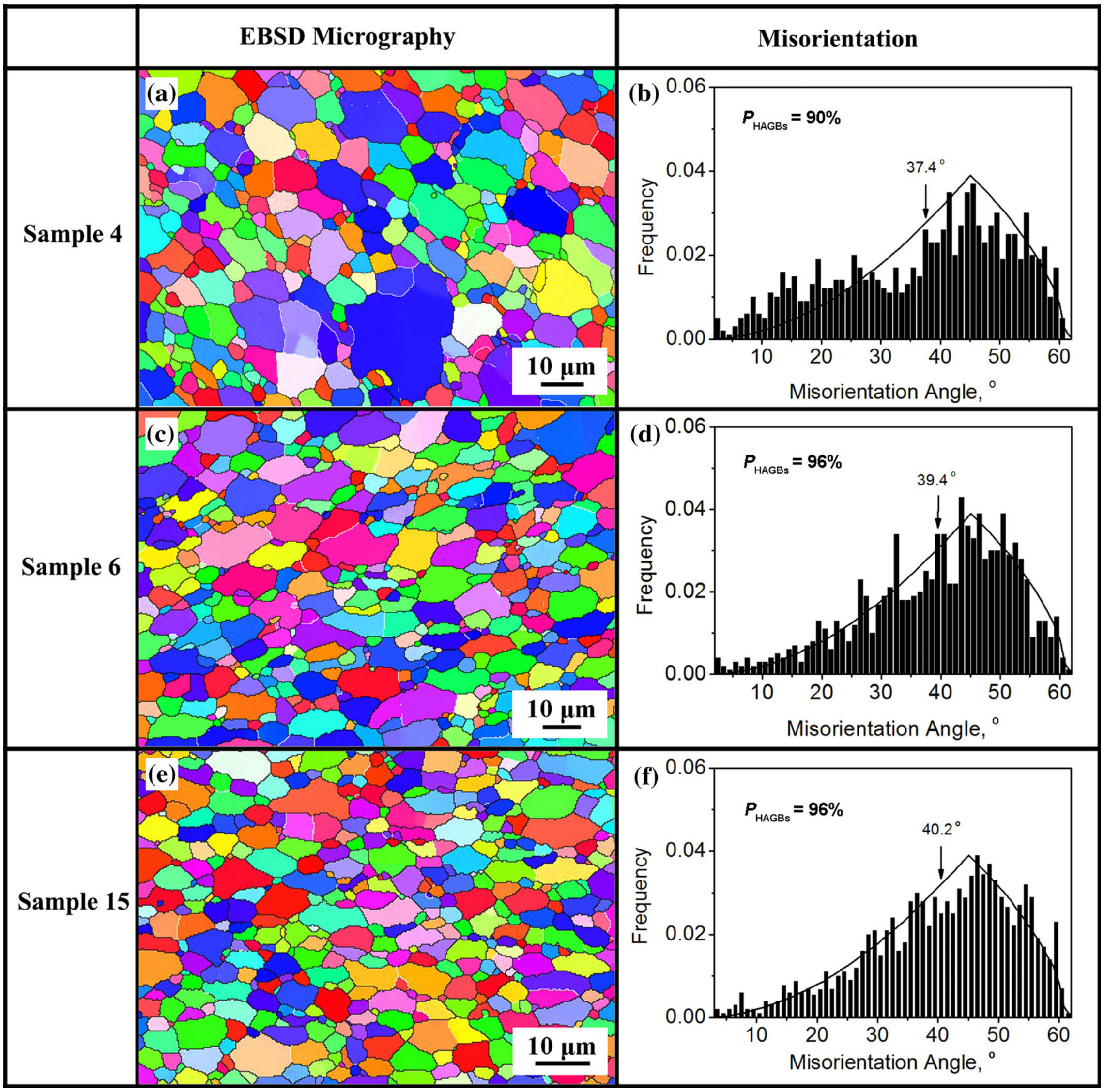

Fig. 7—EBSD micrograph and misorientation distribution for fractured samples.

high superplastic elongation with high m values at high strain rates under relatively low flow stress compared to the samples processed by rolling and ECAP.

C. *Typical Microstructure of the Failed Samples*

The failed samples, samples 4, 6, and 15, were subjected to microstructural examination to understand the microstructural evolution during superplastic deformation for the typical microstructures with a low, medium, and high percentage of HAGBs, respectively. The EBSD maps showed that the microstructure of all the failed samples was characterized by fully recrystallized grains which were somewhat elongated along the tensile direction (Figures 7(a), (c), and (e)). In all the failed samples, the percentage of HAGBs was higher than 90 pct, and the distribution of grain boundary misorientation was close to the random misorientation distribution (Figures 7(b), (d), and (f)). It should be noted that the strong texture (Figures 8(a) and (c)) in samples 4 and 6 was weakened after superplastic deformation (Figures 8(b) and (d)). Sample 15 maintained weak texture during the superplastic deformation (Figures 8(e) and (f)).

IV. DISCUSSION

A. *Superplastic Deformation Mechanism*

The microstructural examinations showed that the largely irregular-shaped grains with many fine equiaxed subgrains in the cold-rolled and ECAP samples (Figures 2(d) and (f)) were replaced by approximately equiaxed grains separated mainly by the HAGBs at high strains (Figures 7(a) and (c)). Correspondingly, the maximum texture intensity also decreased greatly (Figures 8(a) through (d)). Similar microstructural evolutions were

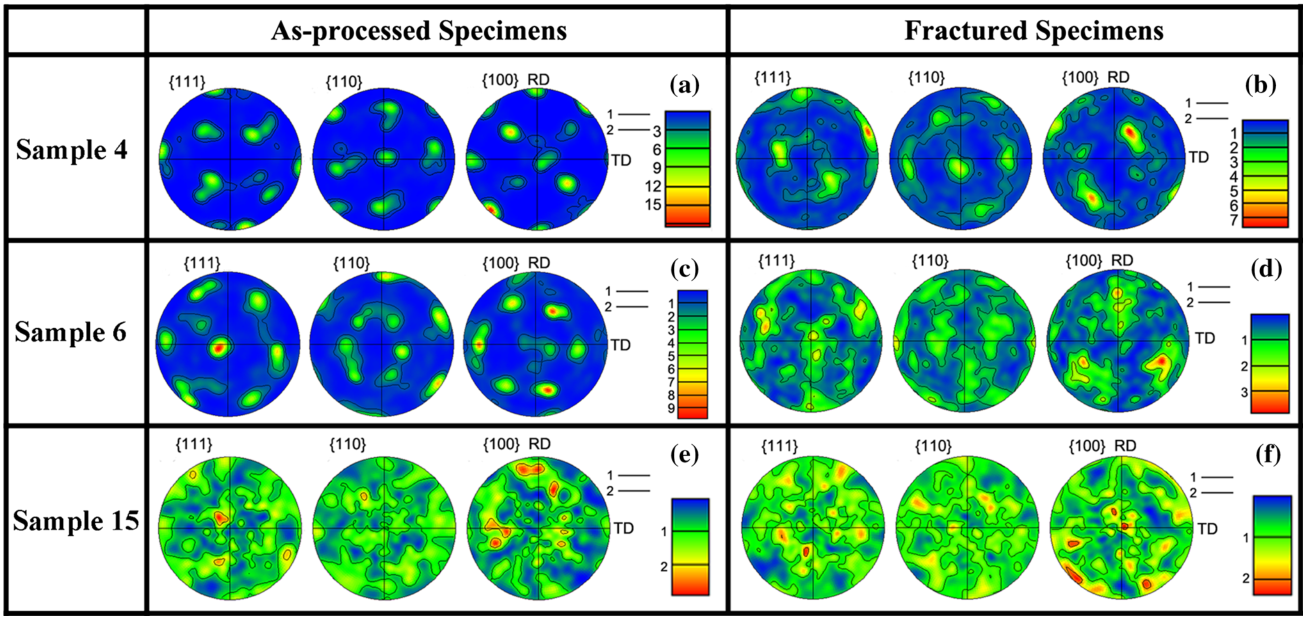

Fig. 8—Pole figures of (*a*) as-processed and (*b*) fractured specimens of sample 4, (*c*) as-processed and (*d*) fractured specimens of samples 6, (*e*) as-processed and (*f*) fractured specimens of sample 15.

also observed in 8090Al,[36] Al-6Cu-0.4Zr,[37] Al-Mg-Sc,[38] and Sc-modified 7050Al,[39] in which the initially deformed structure was replaced by equiaxed grains with a random misorientation distribution after superplastic deformation. Although the mechanism by which the fine-grained structure was obtained is still not absolutely clear, it is generally accepted that both the continuous dynamic recrystallization and GBS took place in the unrecrystallized alloys during superplastic flow.[36–42]

The microstructural examinations revealed that the subgrains developed into approximately equiaxed grains for the cold-rolled and ECAP samples during superplastic deformation, indicating a high contribution of GBS to the deformation and the subgrains being the real GBS units during superplastic deformation. For the samples processed mainly by FSP (samples 7 to 15), the grains retained a random distribution, but the average grain size increased significantly and the grains were somewhat elongated along the tensile direction after superplastic deformation (Figure 7(e)). The misorientation distribution remained almost unchanged and matched well with the theoretical distribution. A very weak, almost random texture was observed in both the undeformed and deformed samples. This microstructural evolution clearly demonstrated that the main deformation mechanism of the FSP Al-Mg-Sc during superplastic deformation is GBS.

Besides the microstructural evolution, the precise evaluation of the parametric dependencies is also important for identifying the superplastic deformation mechanism. In this study, the m values were lower than 0.5 for the samples processed by rolling and ECAP (samples 1 to 6). The lower m values might not represent a genuine change in the deformation mechanism, but rather originate from the existence of a threshold stress. Employing an extrapolation of data to the zero strain rates with a linear regression method in a double linear plot of σ with $\dot{\varepsilon}^{1/2}$ shows the existence of threshold stresses in the samples processed by rolling and ECAP (Figures 9(a) and (c)). After subtracting out the threshold stress from the flow stress, the true m values were close to 0.5 for these samples.

In order to determine the true activation energy for the superplastic deformation, the temperature dependence of flow stress at a constant strain rate is shown in Figures 9(b), (d), and (f). The true activation energies were determined to be 81, 88, and 80 kJ/mol for typical samples 4, 6, and 15, respectively. These activation energies are close to that for the grain boundary diffusion of Al alloy (84 kJ/mol). This is different from the high activation energies detected in ultrafine-grained Al alloys[11] in which the activation energies are close to that for the lattice self-diffusion in pure Al (142 kJ/mol) owing to the significantly reduced grain size.

In order to further elucidate the superplastic deformation mechanism of the Al-Mg-Sc alloys, the variation of $\dot{\varepsilon}kTd^2/D_gEb^3$ is plotted against $(\sigma - \sigma_0)/E$ in Figure 10. Because the subgrains were the real GBS units, the subgrain size instead of the grain size was used as d in Figure 10 for the samples processed by rolling and ECAP in this study. It is clear that the data fitted into a straight line with a slope of 2 for each sample, showing that the stress dependence of superplastic flow is approximately 2, and the temperature dependence of superplastic flow is similar to the activation energy for the grain boundary self-diffusion of Al. This agrees well with the superplastic data analysis for other fine-grained Al alloys,[20,21,24,43] in which the superplastic deformation was dominated by GBS.

Both the microstructural evolution during superplastic deformation and the superplastic data analysis

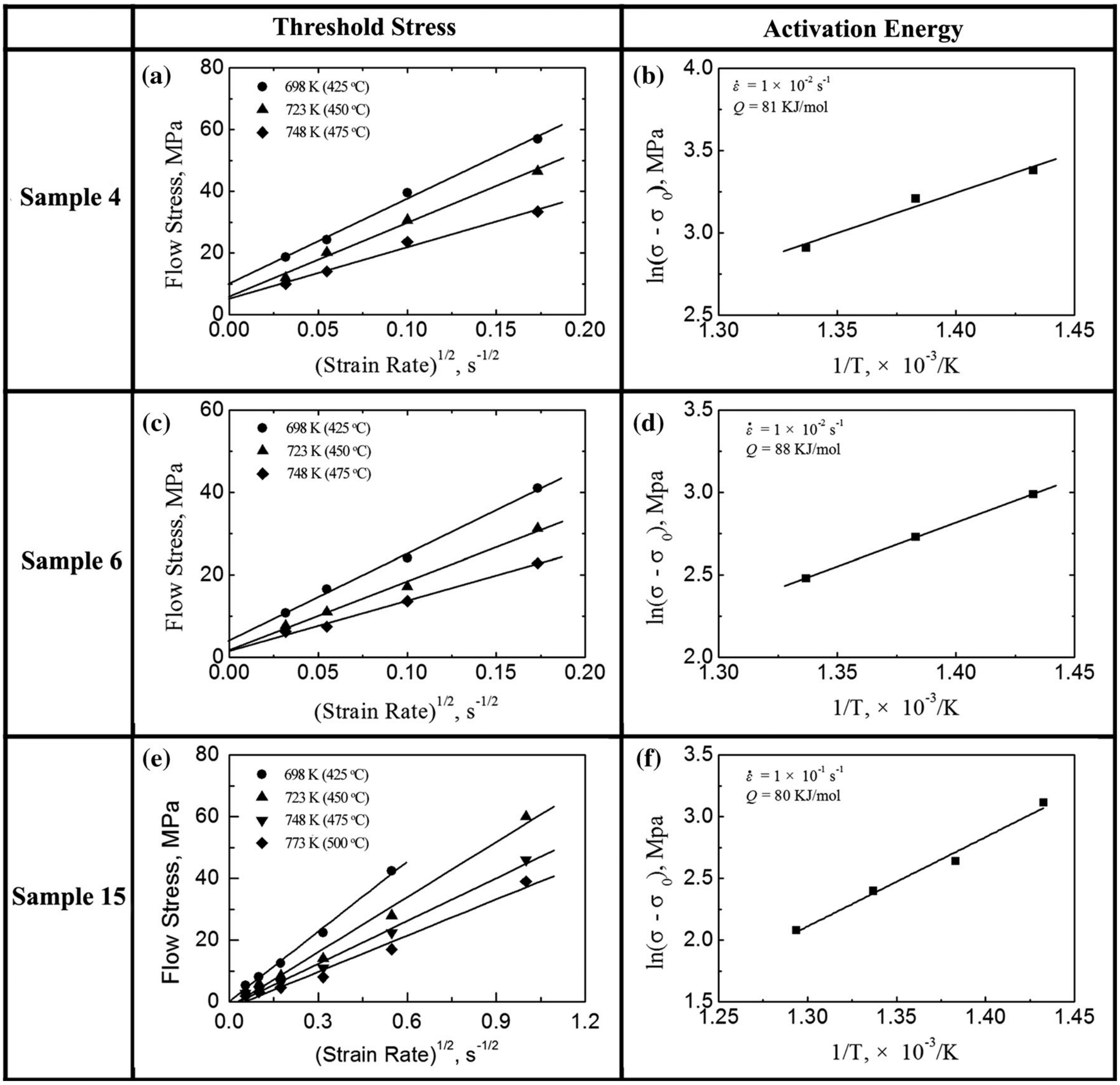

Fig. 9—Threshold stress and activation energy, respectively, for sample 4 (*a*, *b*), sample 6 (*c*, *d*), and sample 15 (*e*, *f*).

indicated that the dominant superplastic deformation mechanism is similar for all the Al-Mg-Sc samples investigated in this study: GBS controlled by grain boundary diffusion. However, the subgrains were the GBS units for the samples processed by TMP and ECAP (samples 1 to 6), in which a high fraction of unrecrystallized deformed structures were observed. The fine grains were the superplastic deformation units for the FSP samples characterized by approximately fully recrystallized grains.

B. *Enhanced Superplastic Deformation Kinetics*

The variation of dimensionless values with the percentage of HAGBs is plotted in Figure 11 for the purpose of clarifying their relationships. The superplastic data obtained in a previous investigation[17] are also included in Figure 11. It is clearly shown that the dimensionless values increased slightly as the percentage of HAGBs was increased in the initial stage, and then increased sharply when the percentage of HAGBs increased past 80 pct. The relationship of dimensionless value (A) and the percentage of HAGBs (P_{HAGBs}) can be approximately expressed by an empirical equation:

$$A = 1.075^{[100 \times P_{\mathrm{HAGBs}}]} \qquad [2]$$

It should be noted that although the value of A was mainly determined by the P_{HAGBs}, other factors, such as the grain shapes and dispersoid distribution, might also have some small impact on the superplastic flow. Therefore, it is not completely unexpected if the data slightly deviate away from Eq. [2].

Based on the discussion above, the steady-state deformation of fine-grained materials at elevated temperatures can be expressed by the following equation:

$$\dot{\varepsilon} = B^{[100 \times P_{\mathrm{HAGBs}}]} \times \frac{D_0 E b}{kT} \exp\left(-\frac{Q}{RT}\right)\left(\frac{b}{d^{\mathrm{eff}}}\right)^2 \left(\frac{\sigma - \sigma_0}{E}\right)^2, \qquad [3]$$

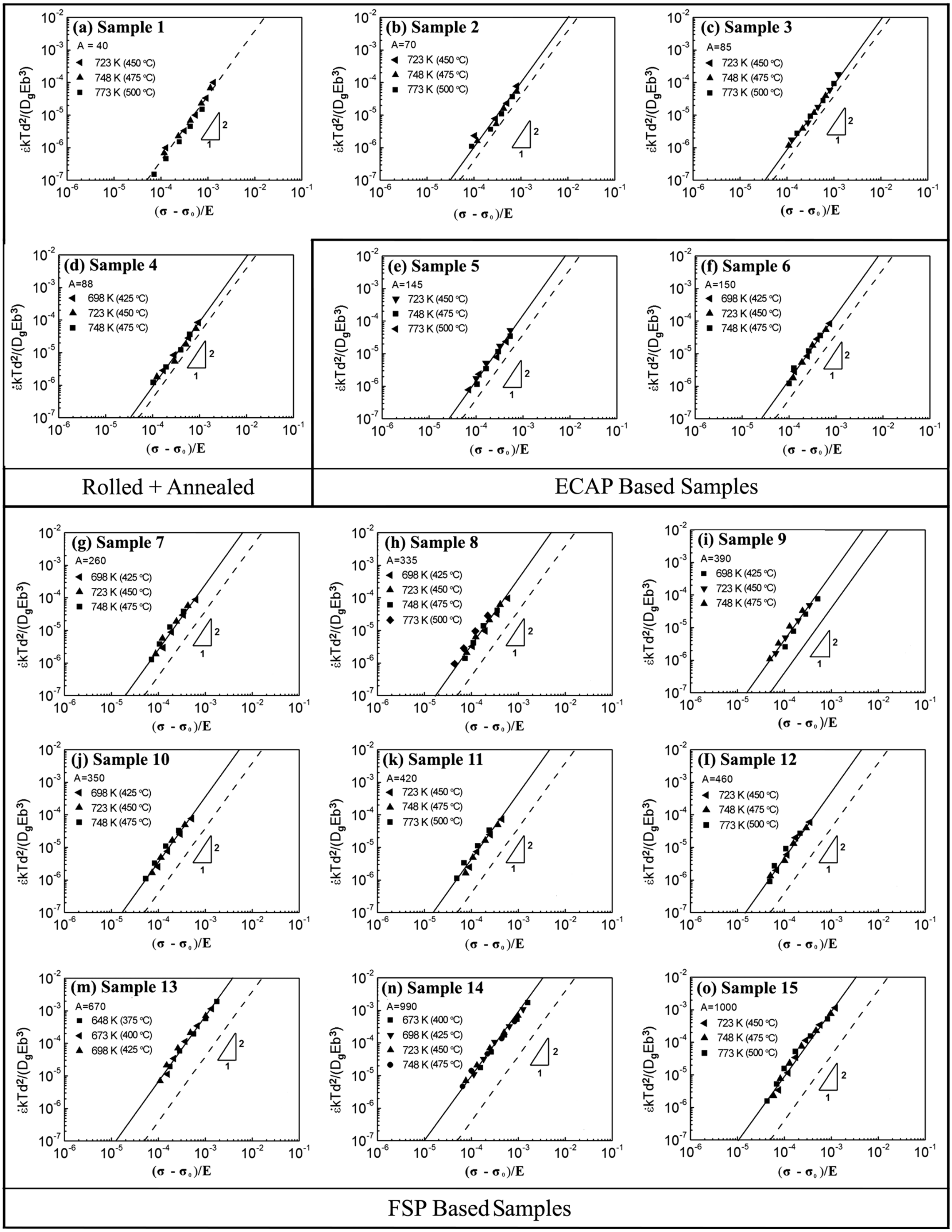

Fig. 10—Variation of $\left(\dot{\varepsilon}kTd^2/D_gEb^3\right)$ as a function of $(\sigma - \sigma_0)/E$ for fine-grained Al-Mg-Sc samples processed by various processing methods.

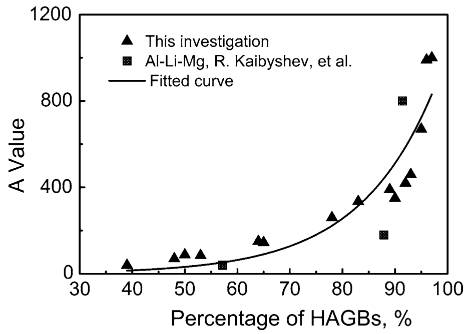

Fig. 11—Variation of A values as a function of the percentage of HAGBs.

where B is a dimensionless value depending on the materials and their preparation processes. For the fine-grained Al alloys processed *via* severe plastic deformation methods, B is roughly equal to 1.075.

Equation [3] shows that the enhanced superplastic deformation kinetics is observed in fine-grained samples which contain a high percentage of HAGBs. This is consistent with the previous reports that the enhanced superplastic deformation kinetics was extensively observed in FSP Al alloys.[20,23,24] The enhanced superplastic deformation kinetics is attractive for practical superplastic forming because it means that (1) the optimum superplastic deformation rate can be shifted to a higher value without reducing the grain size, and (2) a lower flow stress is needed for the samples to be deformed at the same temperature and strain rate.

It is generally accepted that GBS can occur along HAGBs. However, the debates about whether GBS can occur along LAGBs are continuing. A study concerning bicrystals[44] showed that GBS is unlikely to occur between subgrains, owing to minor differences in their orientation. Hales and McNelley[45] suggested that GBS would occur when the boundary misorientation reached about 5 deg to 7 deg. Gudmundsson *et al*.[46] proposed that LAGBs cannot slide at the start of the straining of polycrystalline alloys. Sliding along the pre-existing HAGBs caused the rotation of adjoining subgrains, thereby introducing additional HAGBs which are able to slide. Repetition of this process transformed LAGBs to HAGBs throughout the microstructure.

In this study, the subgrain boundaries in the rolled and ECAP samples transformed into HAGBs after high-strain-rate superplastic deformation under high tensile stress compared to the FSP samples (Figures 5 through 7), and the superplastic deformation mechanism was dominated by GBS. These indicate that the sliding along subgrain boundaries is likely to happen at the early stage of superplastic deformation for the fine-grained Al alloys. It is noted that GBS along HAGBs is easier than that along LAGBs and a lower tensile stress is required to start the sliding along HAGBs. This is why a lower flow stress or an enhanced superplastic deformation kinetics was observed in the fine-grain Al alloys containing high percentages of HAGBs.

The overall implication of the present results is significant. It is shown that for the superplastic constitutive equation of fine-grained Al alloys, in addition to the grain size, the percentage of HAGBs is another important microstructural parameter for the determination of the superplastic properties of fine-grained Al alloys. The modified constitutive equation for superplasticity of fine-grained Al alloys has a wide application. In order to obtain ideal superplasticity, it is necessary to produce fine-grained alloys with both a reduced grain size and an increased percentage of HAGBs.

V. CONCLUSIONS

In order to reveal the origin of the enhanced superplastic deformation kinetics, a series of fine-grained Al alloys with different percentages of HAGBs were prepared by TMP, ECAP, FSP, and their combinations and were then subjected to superplastic investigation. The main conclusions are summarized as follows:

(1) All the fine-grained Al-Mg-Sc samples prepared by TMP, ECAP, FSP, and their combinations exhibited excellent superplasticity. The FSP samples exhibited better superplasticity than those processed by other processing methods because the fine equiaxed grains mostly surrounded by HAGBs in the FSP samples were beneficial to the occurrence of GBS during the superplastic deformation.

(2) The dominant deformation mechanism was the same for all the fine-grained Al-Mg-Sc samples, *i.e.,* grain boundary sliding (GBS) controlled by grain boundary diffusion. However, the subgrains were the GBS units for the TMP or ECAP samples, which contained high percentages of unrecrystallized grains, whereas the fine grains were the GBS units for the FSP samples, characterized by fully recrystallized grains.

(3) The value of dimensionless A used in the classical constitutive equation for superplasticity of fine-grained Al alloys was not a constant, but increased with an increase in the percentage of HAGBs, demonstrating that the enhanced superplastic deformation kinetics was ascribed to the high percentage of HAGBs.

(4) The constitutive equation used to describe superplastic flow was modified to be $\dot{\varepsilon} = B^{[100\times P_{\mathrm{HAGBs}}]} \times \frac{D_0 E b}{kT}\exp\left(-\frac{Q}{RT}\right)\left(\frac{b}{d^{\mathrm{eff}}}\right)^2\left(\frac{\sigma-\sigma_0}{E}\right)^2$, where the percentage of HAGBs (P_{HAGBs}) is another important microstructural parameter in determining superplastic properties.

ACKNOWLEDGMENT

This work was supported by the National Natural Science Foundation of China under Grant Nos. 50871111 and 51331008.

REFERENCES

1. Z.Y. Ma and R.S. Mishra: Friction Stir Superplasticity for Unitized Structures. ISBN: 978-0-12-420006-7, 2014, pp. 1–2.
2. R.S. Mishra, T.R. Bieler, and A.K. Mukherjee: *Acta Mater*., 1997, vol. 45, pp. 561–68.
3. M. Mabuchi and K. Higashi: *Int*. *J*. *Plast*, 2001, vol. 17, pp. 399–407.
4. A. Arieli and A.K. Mukherjee: *Mater*. *Sci*. *Eng*., 1980, vol. 45, pp. 61–70.
5. T.G. Langdon: *Acta*. *Metall*. *Mater*., 1994, vol. 42, pp. 2437–43.
6. R.S. Mishra and Z.Y. Ma: *Mater*. *Sci*. *Eng*. *R*, 2005, vol. 50, pp. 1–78.
7. R.Z. Valiev, R.K. Islamgaliev, and I.V. Alexandrov: *Prog*. *Mater*. *Sci*., 2000, vol. 45, pp. 103–89.
8. J. Wang, Y. Iwahashi, Z. Horita, M. Furukawa, M. Nemoto, R.Z. Valiev, and T.G. Langdon: *Acta Mater*., 1996, vol. 44, pp. 2973–82.
9. N.A. Smirnova, V.I. Levit, V.I. Pilyugin, R.I. Kuznetsov, L.S. Davydova, and V.A. Sazonova: *Fiz*. *Metal*. *Metall*., 1986, vol. 61, pp. 1170–77.
10. R. Kaibyshev, E. Avtokratova, A. Apollonov, and R. Daives: *Scripta Mater*., 2006, vol. 54, pp. 2119–24.
11. Z.Y. Ma, F.C. Liu, and R.S. Mishra: *Acta Mater*., 2010, vol. 58, pp. 4693–4704.
12. R.Z. Valiev, D.A. Salimonenko, N.K. Tsenev, P.B. Berbon, and T.G. Langdon: *Scripta Mater*., 1997, vol. 37, pp. 1945–50.
13. F.C. Liu, Z.Y. Ma, and L.Q. Chen: *Scripta Mater*., 2009, vol. 60, pp. 968–71.
14. J.N. Wang and Y. Wang: *Int*. *J*. *Plast*., 2006, vol. 22, pp. 1530–48.
15. Z. Horita, M. Furukawa, M. Nemoto, A.J. Barnes, and T.G. Langdon: *Acta Mater*., 2000, vol. 48, pp. 3633–40.
16. F.C. Liu and Z.Y. Ma: *Scripta Mater*., 2008, vol. 59, pp. 882–85.
17. R. Kaibyshev, K. Shipilova, F. Musin, and Y. Motohashi: *Mater*. *Sci*. *Technol*., 2005, vol. 21, pp. 408–18.
18. R.S. Mishra, M.W. Mahoney, S.X. McFadden, N.A. Mara, and A.K. Mukherjee: *Scripta Mater*., 1999, vol. 42, pp. 163–68.
19. Z.Y. Ma, R.S. Mishra, M.W. Mahoney, and R. Grimes: *Mater*. *Sci*. *Eng*. *A*, 2003, vol. 35, pp. 148–53.
20. Z.Y. Ma, R.S. Mishra, and M.W. Mahoney: *Acta Mater*., 2002, vol. 50, pp. 4419–30.
21. Z.Y. Ma, R.S. Mishra, M.W. Mahoney, and R. Grimes: *Metall*. *Mater*. *Trans*. *A*, 2005, vol. 36A, pp. 1447–58.
22. X.G. Jiang, J.Z. Cui, and L.X. Ma: *Acta Metall*. *Mater*., 1993, vol. 41, pp. 2721–27.
23. F.C. Liu and Z.Y. Ma: *J*. *Mater*. *Sci*., 2009, vol. 44, pp. 2647–55.
24. F.C. Liu and Z.Y. Ma: *Mater*. *Sci*. *Eng*. *A*, 2011, vol. 530, pp. 548–58.
25. F.C. Liu, Z.Y. Ma, and F.C. Zhang: *J*. *Mater*. *Sci*. *Technol*., 2012, vol. 28, pp. 1025–30.
26. J.Q. Su, T.W. Nelson, and C.J. Sterling: *Philos*. *Mag*., 2006, vol. 86, pp. 1–24.
27. M. Eddahbi, O.A. Ruano, and T.R. McNelley: *Metall*. *Mater*. *Trans*. *A*, 2001, vol. 32A, pp. 1093–1102.
28. T. McNelley and M. McMahon: *Metall*. *Mater*. *Trans*. *A*, 1997, vol. 28A, pp. 1879–87.
29. O. Sitdikov, T. Sakai, E. Avtokratova, R. Kaibyshev, K. Tsuzaki, and Y. Watanabe: *Acta Mater*., 2008, vol. 56, pp. 821–34.
30. O. Sitdikov, T. Sakai, E. Avtokratova, R. Kaibyshev, Y. Kimura, and K. Tsuzaki: *Mater*. *Sci*. *Eng*. *A*, 2007, vol. 444, pp. 18–30.
31. F.J. Humphreys: *J*. *Mater*. *Sci*., 2001, vol. 36, pp. 3833–54.
32. R.Z. Valiev and T.G. Langdon: *Prog*. *Mater Sci*., 2006, vol. 51, pp. 881–981.
33. J.K. Mackenzie: *Biometrica*, 1958, vol. 45, pp. 229–40.
34. M. Ferry and N. Burhan: *Acta Mater*., 2007, vol. 55, pp. 3479–91.
35. S. Komura, P.B. Berbon, M. Furukawa, Z. Horita, M. Nemoto, and T.G. Langdon: *Scripta Mater*., 1998, vol. 38, pp. 1851–56.
36. P.S. Bate, N. Ridley, and B. Zhang: *Acta Mater*., 2007, vol. 55, pp. 4995–5006.
37. P.S. Bate, F.J. Humphreys, N. Ridley, and B. Zhang: *Acta Mater*., 2005, vol. 53, pp. 3059–69.
38. F.C. Liu, P. Xue, and Z.Y. Ma: *Mater*. *Sci*. *Eng*. *A*, 2012, vol. 547, pp. 55–63.
39. J. Liu and D.J. Chakrabarti: *Acta Mater*., 1996, vol. 44, pp. 4647–61.
40. T.G. Nieh, L.M. Hsiung, J. Wadsworth, and R. Kaibyshev: *Acta Mater*., 1998, vol. 46, pp. 2789–2800.
41. X.Y. Yang, H. Miura, and T. Sakai: *Mater*. *Trans*., 2002, vol. 43, pp. 2400–07.
42. E.W. Lee and T.R. McNelley: *Mater*. *Sci*. *Eng*., 1987, vol. 93, pp. 45–55.
43. L.B. Johannes and R.S. Mishra: *Mater*. *Sci*. *Eng*. *A*, 2007, vol. 464, pp. 255–60.
44. P. Lagard and M. Biscondi: *Can*. *Metal*. *Q*., 1974, vol. 13, pp. 245–51.
45. S.J. Hales and T.R. McNelley: *Acta Metall*., 1988, vol. 36, pp. 1229–39.
46. H. Gudmundsson, D. Brooks, and J.A. Wert: *Acta Metall*. *Mater*., 1991, vol. 39, pp. 19–35.